

# Astrometry of the Neptune-Triton System

Altair Ramos Gomes Júnior

August 24, 2016

## Introduction

In this report I present the preliminary results of the astrometric reductions of the images from the Observatório do Pico dos Dias (OPD) in Brazil. The aim is to obtain precise positions for the Neptune - Triton system and to investigate the orbit of Neptune alone around the Sun. The telescopes used were the Perkin-Elmer (160) with a diameter of 1.6m, the Boller & Chivens (IAG) with a diameter of 0.6m, and the Zeiss telescope with a diameter of 0.6m.

The observations were carried out since 1992 when a CCD big enough was installed in the OPD. The planet and satellite have been constantly observed, and still are, by our group. There were many CCDs (IKON, IXON, CCD101, CCD106, ...) and many filters (V, R, I, No Filter, ...) utilized.

There was more than 5000 images from June 1992 to September 2015. Many of the oldest images had no coordinates in header or they were wrong. Sometimes the filter was missing. Many nights had two exposure sets. The first one with low exposure times so Neptune was not saturated, but there were few reference stars in the field. The second one with higher exposure time so Triton was brighter and had more reference stars than with the the previous exposure, but the image of Neptune were saturated.

In Table 1 it is summarized the final number of images for Neptune (short-exposure observations) and Triton (all observations) for the 3 telescopes. It is also shown the number of positions where Neptune and Triton were identified automatically in the same image (short-exposure observations for precision premium).

**Table 1:** Number of positions by object by telescope

Telescope	Neptune	Triton	Matches
160	782	1341	768
IAG	3162	3645	2909
Zeiss	354	479	341
Total	4298	5465	4018

Number of positions identified of Neptune and Triton by telescope. Matches: Number of positions where Neptune and Triton were identified automatically in the same image.

Fig. 1 shows the distribution of positions where Neptune and Triton are identified in the same image (short-exposure observations) over the years. Figs 2-3 summarizes the distribution of positions with Neptune and Triton in the same image by filter obtained in the Perkin-Elmer and Boller & Chivens telescopes, respectively. Zeiss only has images observed in Clear and I filters.

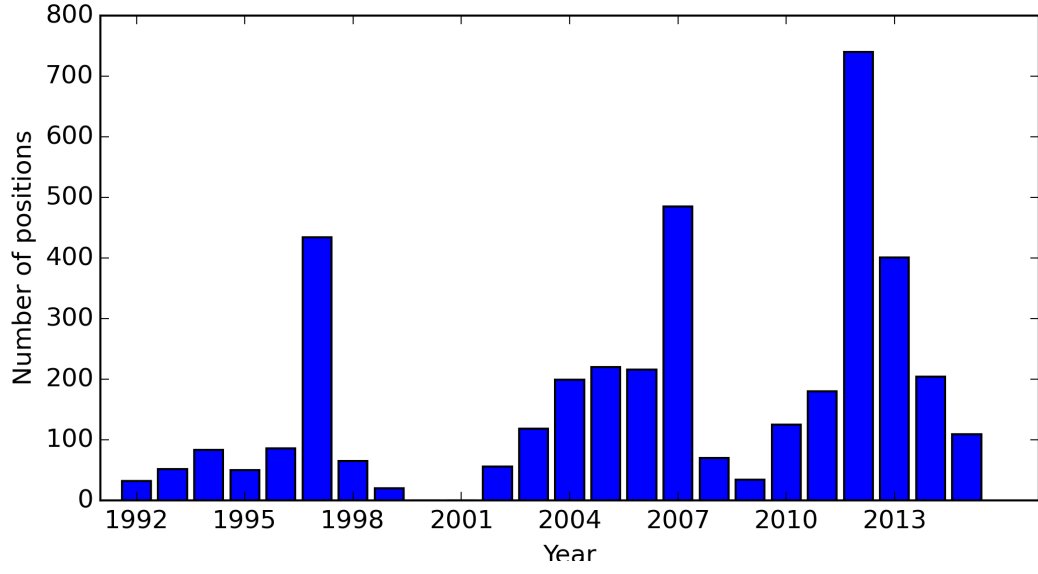


**Figure 1:** Distribution of positions with Neptune and Triton in the same image (short-exposure observations) by year.

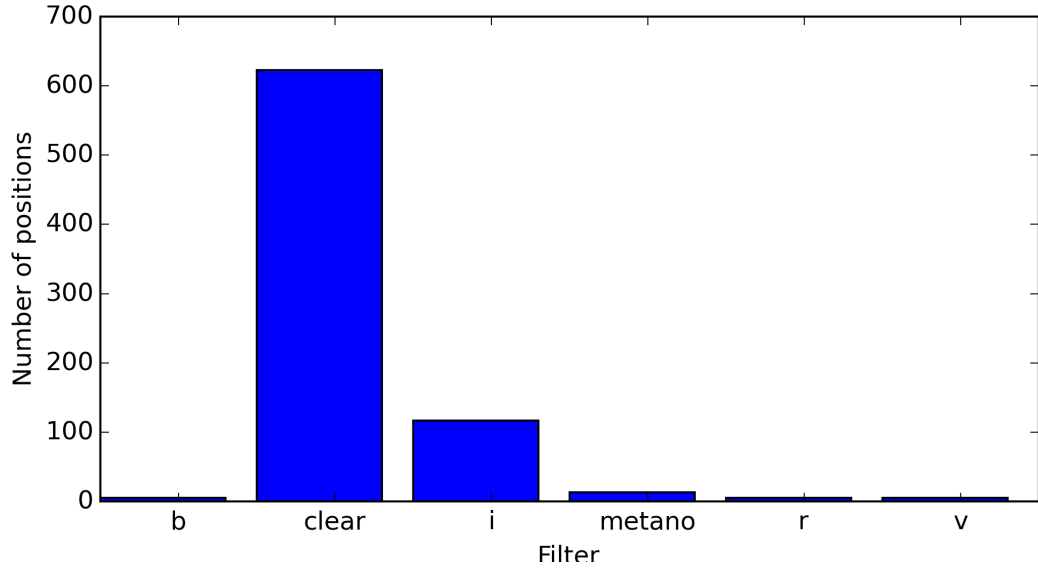


**Figure 2:** Distribution of positions with Neptune and Triton in the same image (short-exposure observations) by filter for the Perkin-Elmer telescope.

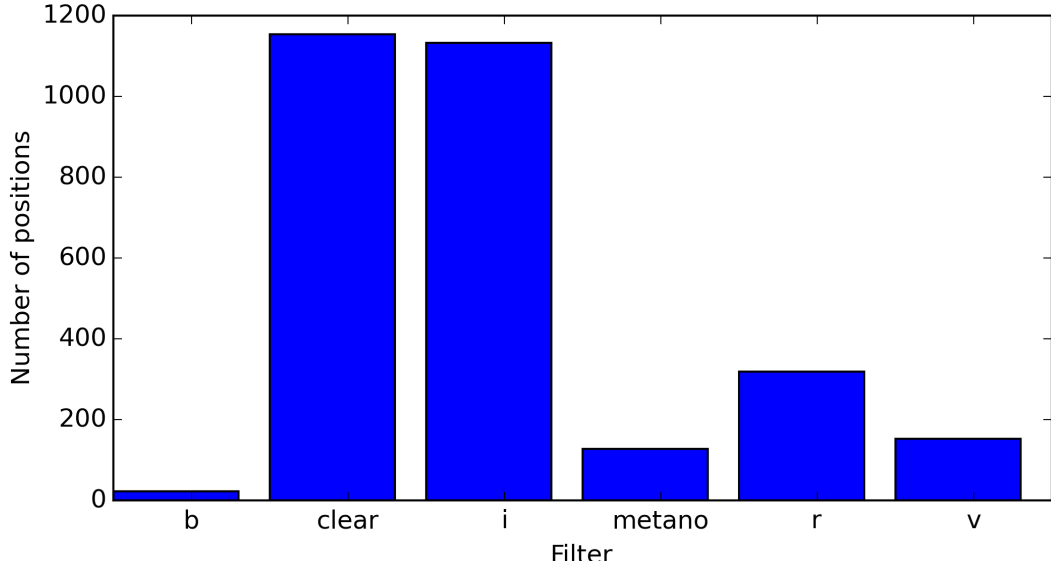


**Figure 3:** Same as in Fig 2 for the Boller & Chivens telescope.

## Reduction

The images were reduced using PRAIA, developed by Marcelo Assafin. To avoid the missing or wrong coordinates I used the coordinates of the ephemeris as input. This way PRAIA could identify reference stars in the images. The reference catalogue used was UCAC4. The ephemeris used to identify Neptune and Triton in the images was DE430+NEP081. The positions where the image of Neptune were saturated and where there were less than 5 reference stars were removed of the results.

In Table 2 it is presented the mean errors in X and Y of the bidimensional Gaussian used to fit the PSF of the objects and the mean value of the dispersion of the offsets by night.

**Table 2:** Table of erros of the reduction. Gaussian error stands for the error in X and Y of the bidimensional Gaussian used to fit the PSF. Mean offset errors is the average dispersion of the positions of each night.

Telescope/Satellite	Gaussian error		Mean offet errors	
	X (mas)	Y (mas)	RA (mas)	DEC (mas)
160/Neptune	$8\pm4$	$8\pm4$	51	39
160/Triton	$14\pm8$	$14\pm8$	35	38
IAG/Neptune	$9\pm7$	$9\pm7$	63	58
IAG/Triton	$20\pm14$	$20\pm14$	52	53
Zeiss/Neptune	$9\pm6$	$9\pm6$	49	57
Zeiss/Triton	$25\pm13$	$25\pm13$	40	51

We applied the digital coronagraphy technique to test if the scattered light of Neptune would influence in the Triton's photocenter. No influence was identified in the 1 mas range.

## Chromatic Refraction Test

Table 3 shows the colors for Triton (Pascu et al., 2006) and Neptune Schmude et al. (2016). Their colors are very different in the blue region. So it is expected that their positions have influence of chromatic refraction with different intensities. The apparent position of Neptune, which is more blue than Triton, would be more shifted towards the zenith than the Triton's position. There may also be noted that in 1992 Neptune had just exited the galactic plane, so the reference stars were redder due to dust.

Object	U-B	B-V	V-R	R-I	V-I
Triton (leading side)		$+0.696 \pm 0.009$			$+0.766 \pm 0.006$
Triton (trailing side)		$+0.699 \pm 0.006$			$+0.776 \pm 0.007$
Neptune	+0.14	+0.39	-0.29	-1.05	+0.76*

**Table 3:** Colors of Triton and Neptune. Leading side is the hemisphere of Triton that is in the direction of its movement. Trailing side is the opposite hemisphere.

\*calculated from V-R and R-I colors.

(Pascu et al., 2006) data also support a secular "blueing" on Triton observed since 1954. They also evidence a reddening episode that happened in 1997 where the B-V color of Triton was bigger than 0.9. A similar reddening was also identified in 1979 (Fig. 4). The authors state that a possible cause of this event is an increase in the activity of geysers.

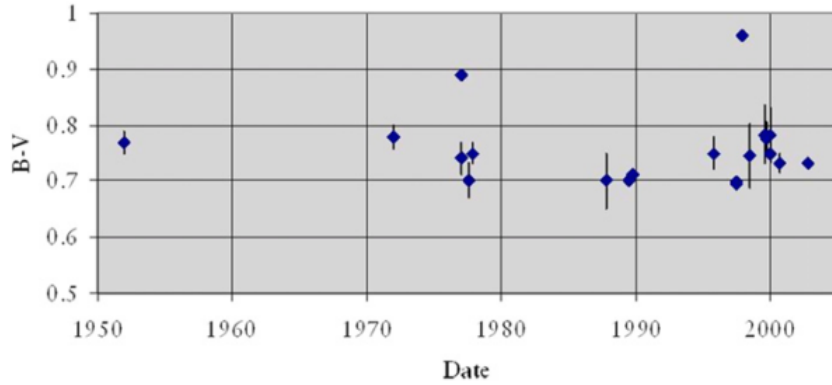
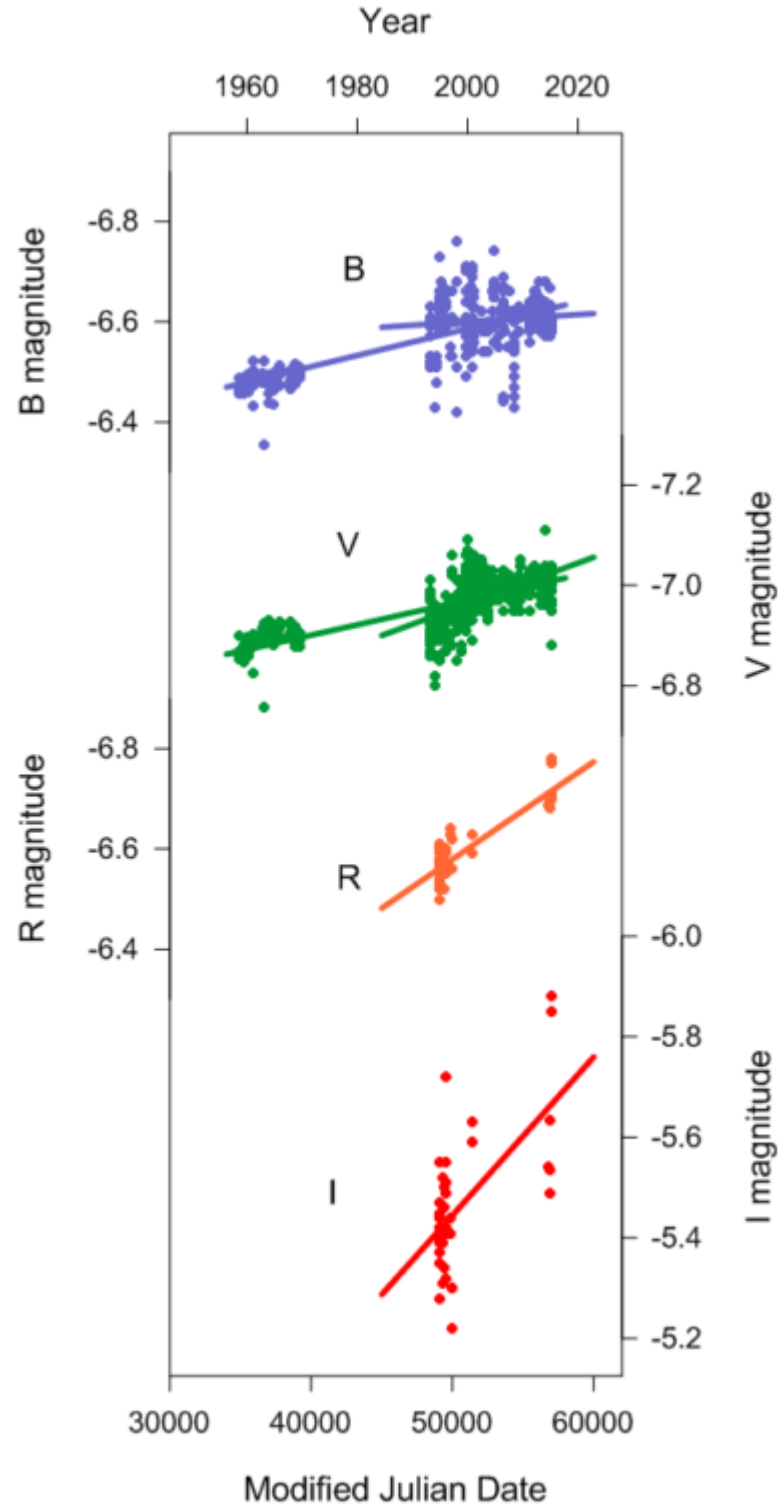


Fig. 1. Summary of  $B-V$  color observations of Triton. Redder colors result in higher values of  $B-V$ . Note the very red colors observed in 1977 and 1997—the latter occurrence only two months after the data reported here (which are among the bluest colors reported). Note that points at 1995.6 and 2002.8 are calculated from reflectance spectra published by Tryka and Bosh (1999) and by Marchi et al. (2004), respectively.

**Figure 4:** Figure extracted from Pascu et al. (2006).

For Neptune, Schmude et al. (2016) showed a secular brightening in the B-, V-, R- and I-bands (Fig. 5) from observations since 1954. They also identified, from Hubble observations, that Neptune has a variation of about 1 magnitude in the I-band over some hours caused by the presence of bright clouds on its atmosphere (Fig. 6). All these circumstances can difficult the estimative of chromatic refraction parameters for Neptune and Triton.



**Figure 5:** Secular brightening of Neptune in B-, V-, R- and I-bands (Schmude et al., 2016).

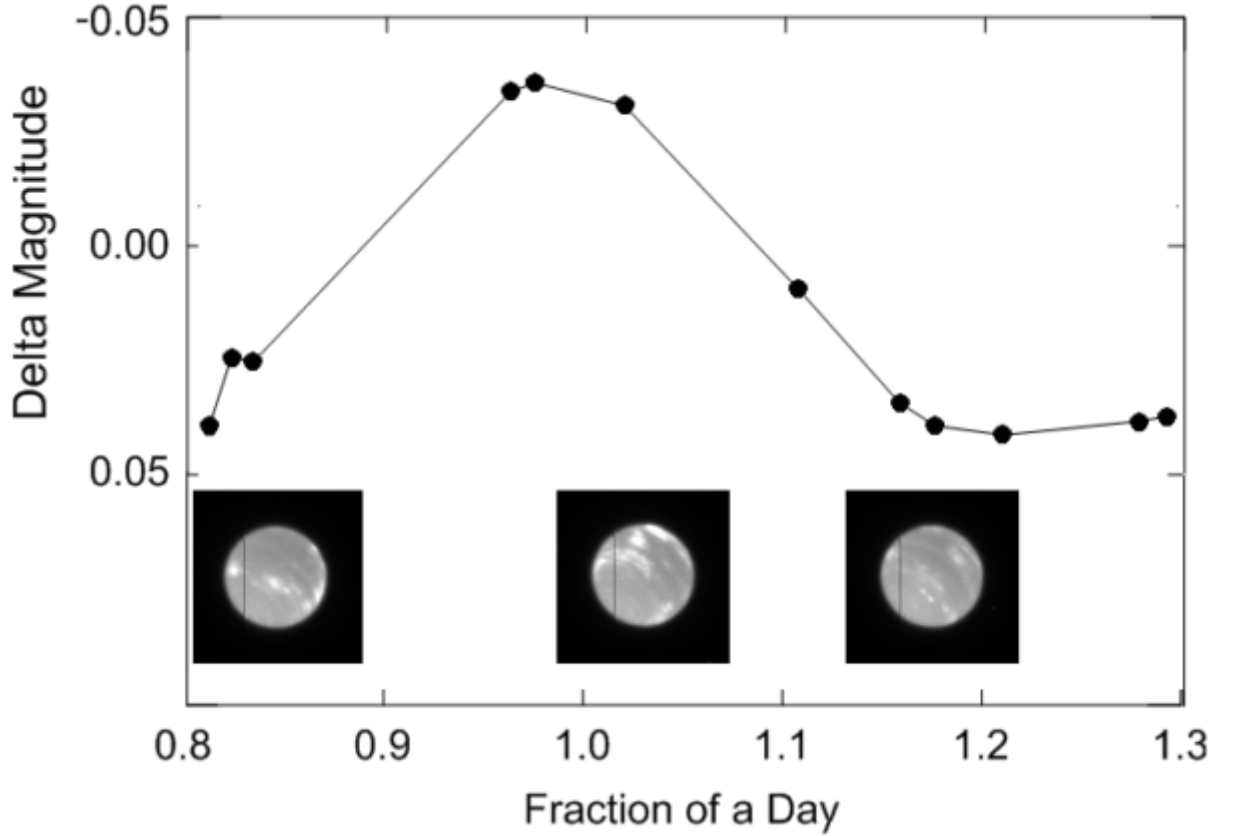


**Figure 6:** HST images of Neptune at  $\lambda = 8450\text{\AA}$  which show a variation of the I-magnitude caused by bright clouds on the atmosphere (Schmude et al., 2016).

To test the effects of chromatic refraction I used the method of Benedetti-Rossi et al. (2014) on all nights with observations distributed over more than 1.5h of hour angle. I used the equation

$$\Delta[\alpha, \delta] = V_{\alpha, \delta}(\phi, \delta, H) \cdot \Delta B, \quad (1)$$

to model the chromatic refraction of the nights.  $\Delta[\alpha, \delta]$  is the position offset for each coordinate  $(\alpha, \delta)$ ,  $V_{\alpha, \delta}(\phi, \delta, H)$  is the first part of refraction which is due to the position of the observed objects and is a function of the latitude of the site ( $\phi$ ), of the object's declination ( $\delta$ ), and of the hour angle ( $H$ ) and  $\Delta B$  is the second part: the differential chromatic refraction which is due to the atmospheric conditions and the wavelength ( $\lambda$ ) of the object and of the stars in the field. This equation is available in Benedetti-Rossi et al. (2014) where it was applied for observations of Pluto.

The model is applied to the offsets in  $\alpha$  and the chromatic parameter  $\Delta B$  is obtained. This parameter is then used to correct the offsets in  $\delta$ .

Figs. 7-10 show the distributions of the offsets in RA and DEC before and after the elimination of chromatic refraction (Neptune-160, Triton-160, Neptune-IAG, Triton-IAG, respectively). Only nights with  $\Delta H > 1.5h$  were used. The histograms clearly show an improvement in the distribution of the offsets, mainly for Neptune. So chromatic refraction is very important and must be removed.

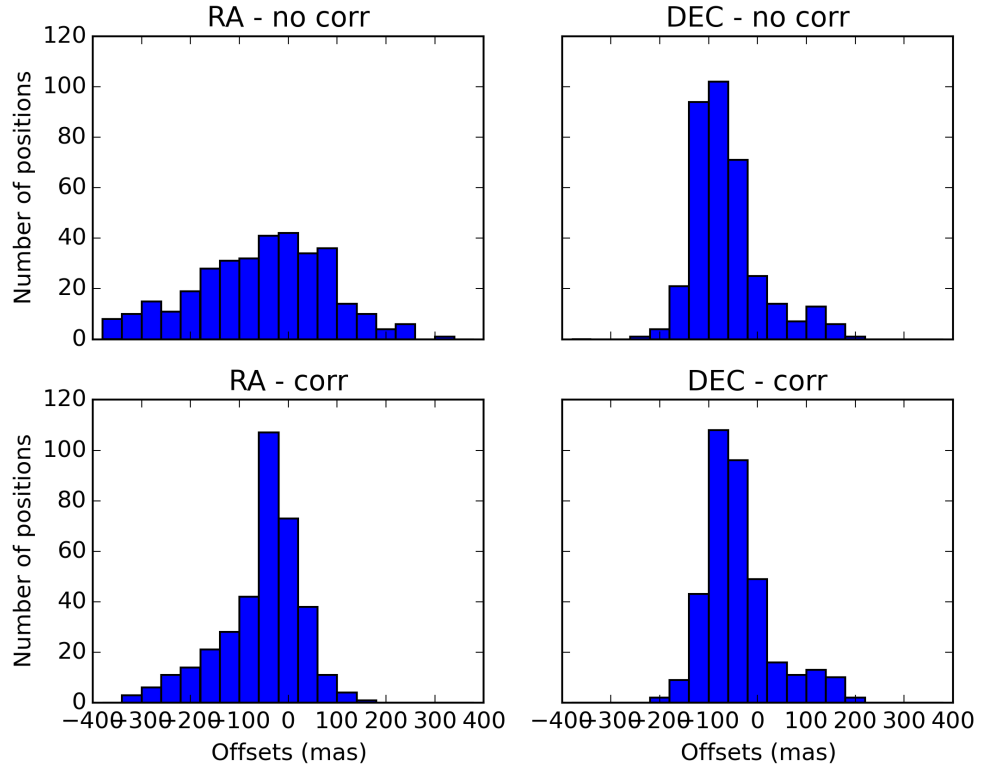


**Figure 7:** Distribution of the offsets of Neptune observed in 160.

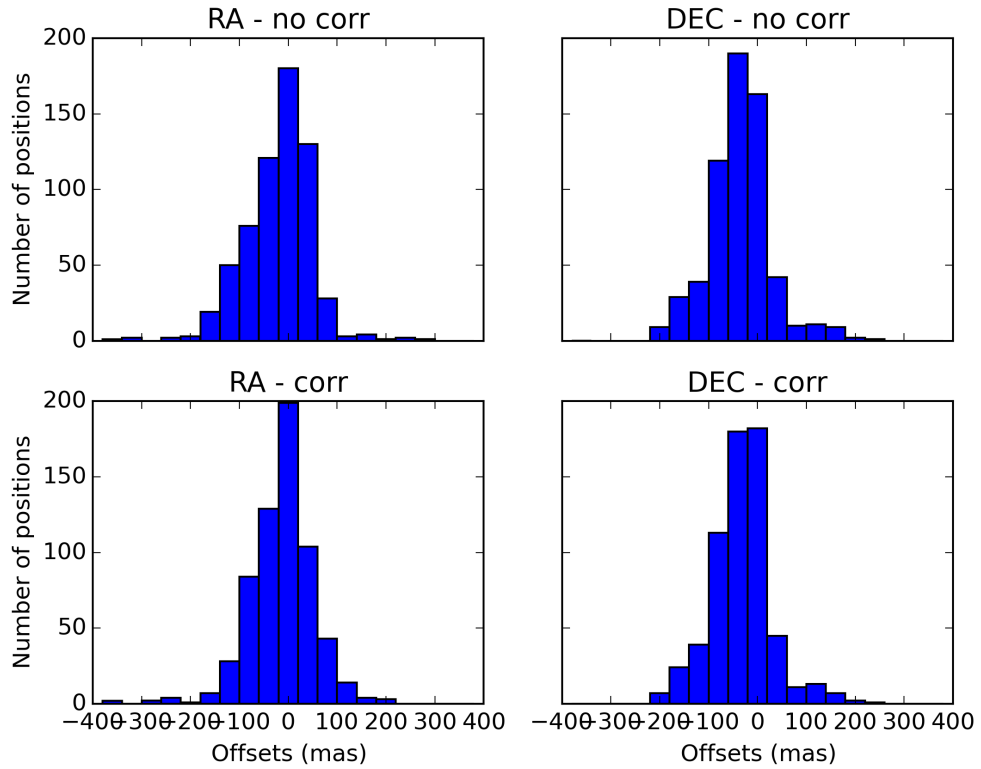


**Figure 8:** Distribution of the offsets of Triton observed in 160.



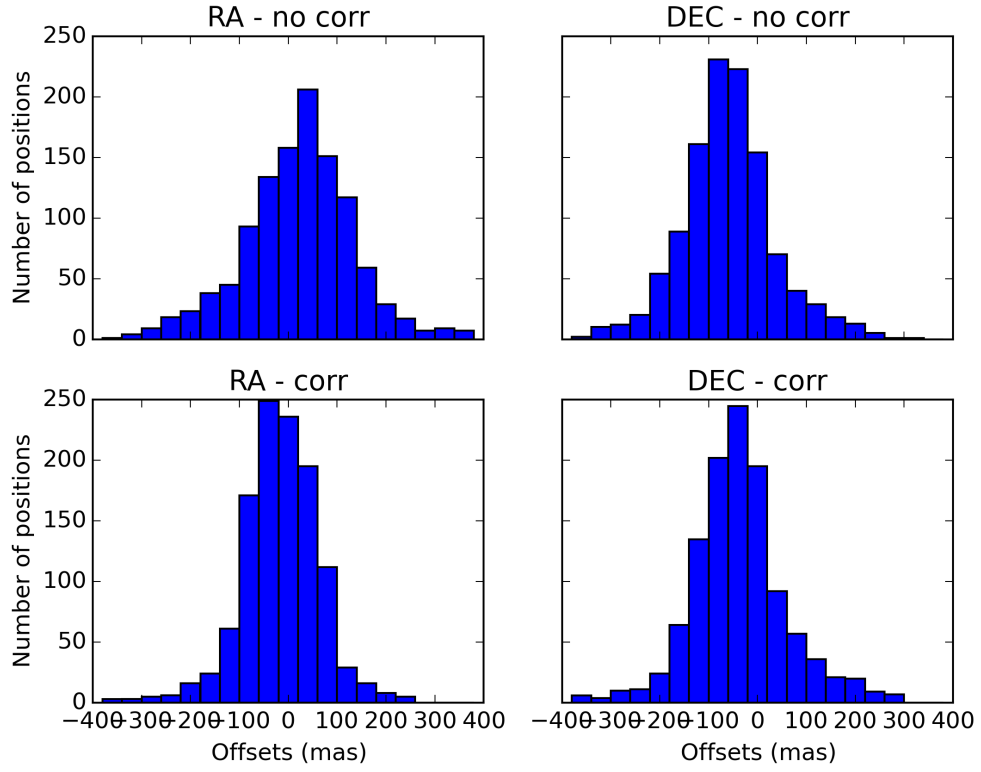


**Figure 9:** Distribution of the offsets of Neptune observed in IAG.

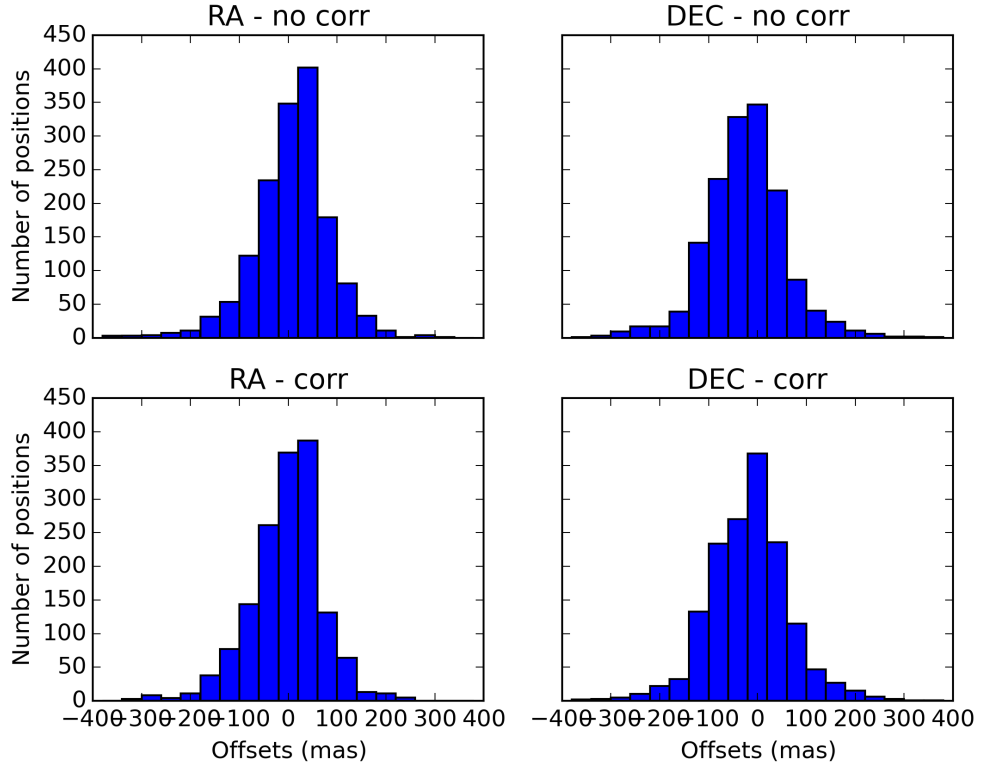


**Figure 10:** Distribution of the offsets of Triton observed in IAG.

Table 4 show respective nights used in the Figs. 7-10, the filter, the variation in hour angle ( $\Delta H$ ), the parameters obtained ( $\Delta B$ ), number of images (Nimg), mean number of reference stars (Nstars) and mean offsets before and after correction. It is possible to see that the  $\Delta B$  calculated has high values for Neptune, while for Triton they are smaller.

For the nights with observations distributed in a smaller time interval, it must be used  $\Delta B$  of close nights observed with the same filter for the correction.

**Table 4:** Obtained parameters and offsets from adjustments. Only nights with  $\Delta H > 1.5h$ .

Neptune-160									
Date	Filter	$\Delta H$	$\Delta B$	Nimg	Nstars	RA no corr	DEC no corr	RA corr	DEC corr
1992-06-09	Clear	1.57	+0.29±0.03	13	11	190± 54	25± 76	-43± 15	65± 68
1992-07-19	Clear	1.63	+0.20±0.04	17	24	50± 46	117± 37	1± 26	125± 36
1993-06-24	Clear	1.61	-0.07±0.04	10	17	-17± 26	-38± 48	-21± 22	-40± 48
1993-06-25	Clear	2.63	+0.03±0.02	12	8	-37± 26	70± 75	-40± 24	72± 74
1993-08-20	Clear	3.35	+0.20±0.02	31	29	15± 76	-83± 43	-7± 34	-75± 44
1993-08-22	Clear	2.87	+0.18±0.02	35	9	-47± 63	-74± 44	-15± 38	-67± 46
1996-06-22	Clear	1.68	+0.24±0.02	19	16	-25± 51	-32± 35	-48± 18	-20± 35
1996-10-02	Clear	1.97	+0.31±0.07	16	6	252±192	-60± 73	-59±126	10± 79
1997-06-01	Clear	4.89	+0.35±0.03	91	11	-155±189	-112± 36	-120±107	-81± 40
1997-06-02	Clear	5.24	+0.22±0.01	60	10	-113±125	-84± 36	-73± 48	-61± 33
1998-06-06	Clear	2.51	+0.38±0.04	35	11	-140±101	-66± 42	-13± 56	-33± 41
1998-09-03	Clear	1.52	+0.30±0.03	20	10	-86± 63	-75± 49	20± 26	-51± 47
Triton-160									
Date	Filter	$\Delta H$	$\Delta B$	Nimg	Nstars	RA no corr	DEC no corr	RA corr	DEC corr
1992-06-09	Clear	1.57	+0.01±0.03	16	16	12± 20	19± 79	3± 20	20± 79
1992-07-19	Clear	1.89	+0.07±0.04	21	25	-3± 33	15± 52	-21± 30	17± 52
1993-06-24	Clear	1.61	+0.01±0.04	15	13	8± 23	15± 55	9± 23	16± 55
1993-06-25	Clear	2.90	-0.09±0.04	20	12	-28± 60	36± 79	-14± 52	32± 80
1993-08-20	Clear	3.35	-0.01±0.02	30	27	-8± 29	-25± 62	-6± 29	-25± 62
1993-08-22	Clear	3.12	+0.05±0.01	43	13	-2± 28	-9± 43	4± 24	-7± 43
1994-09-22	Clear	1.94	-0.12±0.08	13	12	-33± 53	30± 75	48± 49	16± 71

*Continued on next page*

Table 4 – *Continued from previous page*

Date	Filter	$\Delta H$	$\Delta B$	Nimg	Nstars	RA no corr	DEC no corr	RA corr	DEC corr
1994-09-22	Clear	1.55	+0.00±0.04	15	17	-53± 21	24± 82	-54± 21	24± 82
1995-08-07	Clear	3.02	+0.02±0.02	11	21	-10± 14	-40± 30	-10± 13	-39± 30
1996-06-22	Clear	2.28	-0.08±0.02	32	15	-87± 24	-9± 29	-77± 19	-13± 28
1996-08-22	Clear	1.56	+0.01±0.02	29	13	43± 30	-41± 44	37± 30	-40± 44
1996-08-24	Clear	1.99	-0.03±0.04	10	11	46± 15	-66± 23	52± 15	-67± 23
1996-10-02	Clear	1.97	+0.04±0.07	16	6	73±121	1± 76	38±120	9± 77
1997-06-01	Clear	4.89	+0.11±0.01	101	11	-76± 71	-107± 53	-68± 51	-98± 54
1997-06-02	Clear	5.41	+0.02±0.02	81	10	-18± 86	-56± 30	-17± 85	-54± 30
1997-08-11	Clear	3.08	+0.12±0.02	33	11	-30± 46	-23± 27	2± 28	-14± 28
1997-08-13	Clear	1.67	+0.04±0.03	19	6	44± 30	-4± 16	60± 29	-0± 16
1998-06-06	Clear	2.84	+0.13±0.04	42	11	-46± 62	-55± 33	-5± 53	-44± 33
1998-09-03	Clear	1.52	-0.04±0.04	20	10	3± 36	-48± 54	-11± 35	-50± 54
1999-06-06	Clear	1.58	+0.23±0.04	27	14	19± 47	-63± 43	91± 32	-43± 40
1999-08-22	Clear	3.06	+0.03±0.02	30	15	-32± 37	-7± 25	-45± 35	-3± 26
Neptune-IAG									
Date	Filter	$\Delta H$	$\Delta B$	Nimg	Nstars	RA no corr	DEC no corr	RA corr	DEC corr
2001-08-26	B	2.11	+0.15±0.03	44	15	89± 55	-41± 57	14± 41	-22± 57
2002-07-15	Clear	6.11	+0.18±0.00	57	17	51±163	85± 90	-36± 31	131± 76
2002-07-18	Clear	3.86	+0.21±0.02	30	13	-100±115	-140± 61	-50± 61	-111± 61
2003-07-22	Clear	2.38	+0.33±0.04	20	15	174±137	-75± 80	-32± 57	-13± 74
2003-07-23	Clear	4.08	+0.02±0.01	39	16	-81± 36	13± 55	-78± 34	17± 55
2003-07-25	Clear	6.19	-0.01±0.02	21	9	-107± 74	9± 62	-106± 74	7± 62
2003-07-26	Clear	6.97	-0.01±0.08	17	10	-132±211	8±123	-129±211	7±124
2003-07-27	Clear	1.54	+0.06±0.06	26	14	-21±104	4± 84	-90±102	24± 84
2003-07-28	Clear	7.98	+0.01±0.03	43	12	-37±144	21±162	-44±144	24±162
2003-08-20	Clear	4.03	+0.26±0.04	30	17	95±154	-72± 66	18± 98	-35± 60
2003-10-14	V	2.33	+0.02±0.03	8	30	20± 25	16± 31	16± 25	18± 31
2004-08-05	V	2.21	-0.03±0.12	5	6	-53± 67	-61± 25	-35± 67	-66± 26

*Continued on next page*

Table 4 – *Continued from previous page*

Date	Filter	$\Delta H$	$\Delta B$	Nimg	Nstars	RA no corr	DEC no corr	RA corr	DEC corr
2004-08-06	V	3.10	+0.18±0.03	4	6	-160± 61	-173± 60	-165± 14	-151± 59
2004-08-07	V	4.31	+0.21±0.33	6	11	128±333	-40±210	110±317	-9±212
2004-08-21	Clear	4.09	+0.08±0.02	30	21	-32± 57	-78± 55	-56± 44	-66± 57
2004-08-21	Clear	2.57	+0.05±0.02	30	21	-42± 28	-86± 41	-32± 26	-81± 41
2004-08-23	Clear	5.20	+0.06±0.01	70	18	10± 59	-88± 52	-29± 42	-73± 50
2004-08-24	Clear	3.94	+0.06±0.01	40	18	-2± 34	-83± 66	-23± 26	-74± 65
2004-09-24	R	3.08	+0.27±0.05	35	13	157±183	12±136	-0±133	63±126
2004-09-25	Clear	3.75	+0.26±0.03	40	14	201±164	2± 93	37±106	54± 86
2005-09-24	V	2.78	+0.05±0.01	88	14	2± 47	-101± 61	-52± 44	-85± 60
2006-06-08	Clear	2.68	+0.32±0.04	95	24	-91±144	-83± 93	14±115	-30± 93
2011-09-26	I	4.02	+0.05±0.00	250	18	76± 44	-67± 48	38± 36	-52± 45
2012-10-19	R	1.99	+0.13±0.03	119	8	41±100	-167±137	-50± 92	-130±138
Triton-IAG									
Date	Filter	$\Delta H$	$\Delta B$	Nimg	Nstars	RA no corr	DEC no corr	RA corr	DEC corr
2001-08-26	B	2.11	+0.03±0.03	24	15	1± 40	-53± 46	-13± 39	-50± 46
2002-07-15	Clear	6.11	+0.01±0.00	55	17	14± 27	-29± 45	7± 24	-26± 45
2002-07-18	Clear	3.86	-0.01±0.03	31	13	25± 74	-68±111	23± 74	-69±111
2003-07-22	Clear	2.55	+0.08±0.02	31	17	-8± 57	-7± 53	-58± 49	8± 54
2003-07-23	Clear	4.08	+0.04±0.02	38	16	-44± 54	-12± 45	-37± 50	-6± 45
2003-07-25	Clear	6.39	-0.04±0.03	44	16	-60±138	9± 50	-64±136	2± 51
2003-07-26	Clear	6.97	-0.04±0.04	33	14	-133±167	21± 90	-121±165	13± 91
2003-07-27	Clear	1.54	+0.01±0.05	26	14	-31± 76	31± 74	-40± 76	34± 74
2003-07-28	Clear	7.98	-0.01±0.02	60	14	-51±130	46±133	-44±130	43±133
2003-08-20	Clear	4.20	+0.02±0.02	49	21	53± 69	-8± 45	46± 68	-5± 45
2003-10-14	V	3.63	-0.04±0.03	20	33	-4± 54	-34± 72	13± 53	-40± 74
2003-10-15	V	2.27	+0.01±0.05	18	33	-22± 38	-3± 78	-23± 38	-2± 77
2003-10-16	V	1.94	-0.10±0.10	8	25	-18± 64	-15± 36	46± 58	-32± 32
2003-10-17	V	2.09	+0.02±0.04	10	29	1± 31	4± 92	-7± 31	7± 92

*Continued on next page*

Table 4 – *Continued from previous page*

Date	Filter	$\Delta H$	$\Delta B$	Nimg	Nstars	RA no corr	DEC no corr	RA corr	DEC corr
2003-10-19	V	1.89	-0.12 $\pm$ 0.05	12	31	-7 $\pm$ 40	-45 $\pm$ 35	44 $\pm$ 32	-60 $\pm$ 32
2004-08-05	V	2.38	-0.06 $\pm$ 0.02	21	15	-13 $\pm$ 31	-101 $\pm$ 35	21 $\pm$ 26	-111 $\pm$ 35
2004-08-06	V	3.27	+0.06 $\pm$ 0.07	22	16	53 $\pm$ 99	-110 $\pm$ 50	45 $\pm$ 97	-102 $\pm$ 50
2004-08-07	V	4.50	+0.00 $\pm$ 0.03	23	19	54 $\pm$ 56	-117 $\pm$ 61	54 $\pm$ 56	-117 $\pm$ 61
2004-08-20	Clear	3.81	+0.03 $\pm$ 0.01	16	24	-5 $\pm$ 26	-40 $\pm$ 24	-15 $\pm$ 23	-35 $\pm$ 23
2004-08-21	Clear	4.09	+0.02 $\pm$ 0.02	27	22	-13 $\pm$ 41	-32 $\pm$ 52	-22 $\pm$ 39	-28 $\pm$ 53
2004-08-21	Clear	2.57	+0.01 $\pm$ 0.02	26	21	-13 $\pm$ 28	-51 $\pm$ 35	-12 $\pm$ 27	-51 $\pm$ 35
2004-08-23	Clear	5.20	+0.02 $\pm$ 0.01	43	18	-2 $\pm$ 44	-36 $\pm$ 49	-11 $\pm$ 42	-32 $\pm$ 49
2004-08-24	Clear	3.94	+0.02 $\pm$ 0.01	29	17	-2 $\pm$ 29	-34 $\pm$ 62	-9 $\pm$ 28	-31 $\pm$ 62
2004-09-24	R	3.08	+0.04 $\pm$ 0.04	37	14	26 $\pm$ 111	83 $\pm$ 131	2 $\pm$ 109	91 $\pm$ 130
2004-09-25	Clear	3.75	+0.01 $\pm$ 0.04	36	14	59 $\pm$ 113	91 $\pm$ 77	51 $\pm$ 113	93 $\pm$ 77
2005-09-24	V	2.78	+0.01 $\pm$ 0.01	155	16	-14 $\pm$ 43	-95 $\pm$ 56	-26 $\pm$ 43	-91 $\pm$ 56
2006-06-08	Clear	3.30	+0.10 $\pm$ 0.03	157	26	-22 $\pm$ 104	-47 $\pm$ 69	2 $\pm$ 100	-32 $\pm$ 69
2009-07-22	Clear	2.19	+0.08 $\pm$ 0.07	17	15	10 $\pm$ 43	74 $\pm$ 96	-1 $\pm$ 41	87 $\pm$ 95
2011-09-05	I	1.82	+0.19 $\pm$ 0.03	100	18	91 $\pm$ 47	-1 $\pm$ 34	36 $\pm$ 38	38 $\pm$ 36
2011-09-26	I	4.02	-0.00 $\pm$ 0.00	250	18	43 $\pm$ 28	4 $\pm$ 41	43 $\pm$ 28	3 $\pm$ 41
2012-10-19	R	1.99	+0.13 $\pm$ 0.03	118	8	14 $\pm$ 108	-76 $\pm$ 134	-78 $\pm$ 100	-38 $\pm$ 136

## PSF for extended object Test

PRAIA uses a bidimensional circular gaussian fit for the PSF of the objects in the images to obtain their photocenters. But in the case of Neptune, its size is bigger than 2 arcsec, which is comparable to the observational seeing. In this case a gaussian fit may not represent with enough accuracy the PSF of Neptune.

In order to obtain a PSF for extended objects (objects with sizes in the order of the seeing), Vieira-Martins (priv. comm.) obtained the following equation:

$$F_c(x, y) = A \sqrt{\frac{\pi}{2}} \sigma \int_{-R}^{+R} e^{-\frac{(x-x_0-\mu)^2}{2\sigma^2}} \left[ \operatorname{erf} \left( \frac{y-y_0+\sqrt{R^2-\mu^2}}{\sqrt{2}\sigma} \right) - \operatorname{erf} \left( \frac{y-y_0-\sqrt{R^2-\mu^2}}{\sqrt{2}\sigma} \right) \right] d\mu \quad (2)$$

where  $\operatorname{erf}(x)$  is the Error Function defined as:

$$\operatorname{erf}(x) = \frac{2}{\sqrt{\pi}} \int_0^x e^{-t^2} dt \quad (3)$$

The flux  $F_c$  obtained for a given position  $(x, y)$  is obtained by integrating an homogeneous disk where every bit of the disk can be represented by a bidimensional circular Gaussian fit. The parameters to be determined are the amplitude  $A$  and the dispersion  $\sigma$  of the original Gaussian, the center of the disk  $(x_0, y_0)$  and the radius of the disk  $R$ .

Fig. 11 shows the first test with this PSF for a image of Neptune. The image test was taken at OPD in June 08, 2013. The image has a pixel scale of 0.177"/px, an exposure time of 5s and was observed with a B filter.

In this example, the photocenter calculated was different from PRAIA's by 0.01px or 1.77mas. We must still estimate the best region of the image to fit the PSF. We must also test it for other nights.

This test was made using the Scipy packages: Odrpack (for non-linear least square fit) and Special (for the error function). It is possible to see that the function for extended objects (green) fits better the profile of Neptune.

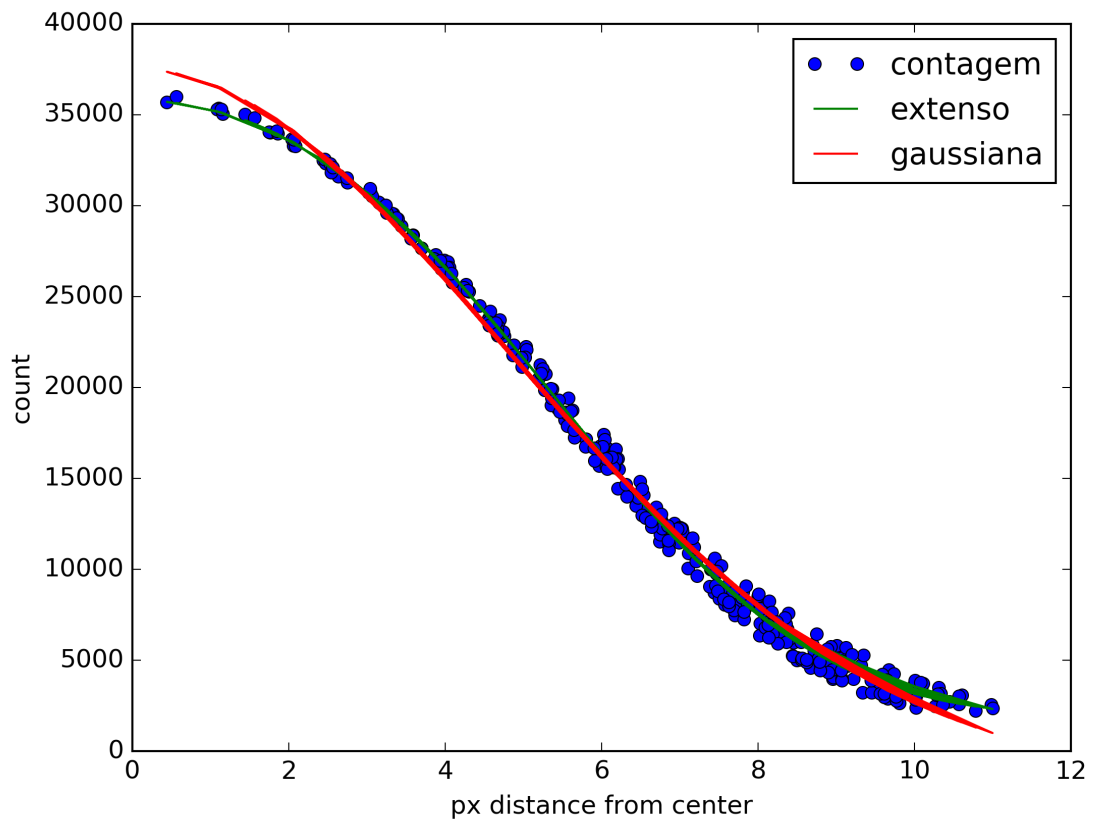
## Final Remarks

Fig 12 shows the mean offsets of each night and respective discrepancy (error bars) for Neptune in RA and DEC, respectively.

Fig 13 shows the difference in the mean offsets night by night for all matched nights and not eliminated by the sigma-clip procedure in the sense Triton - Neptune. The error bars are the mean value of the dispersions in the night for each satellite.

It seems that there are long term systematic errors in the orbit of Neptune, and in the orbit of Triton around Neptune, but it is too soon to state that with confidence. We must still further refine the positions. We plan to do the following:

- Test the PSF for Neptune to identify the best way to reduce all images.
- Utilize an astrometry which uses the same stars in all fields of a night to have a cleaner reduction to eliminate chromatic refraction.
- Further refinements in the data may be needed as we further investigate these position sets.



**Figure 11:** Fit of an image of Neptune with a gaussian fit (red) and with the PSF for extended objects (green).

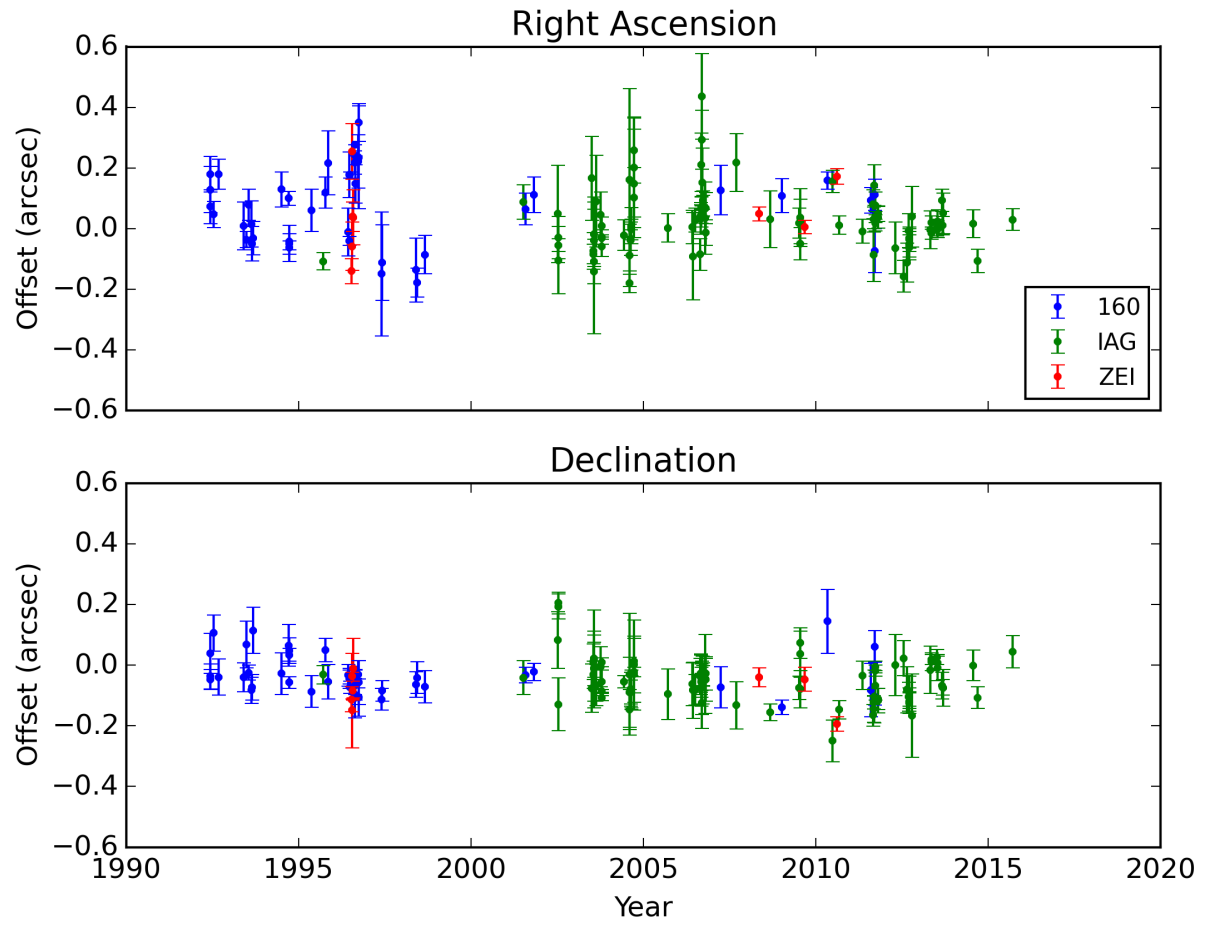


**Figure 12:** Neptune - Mean offsets by day



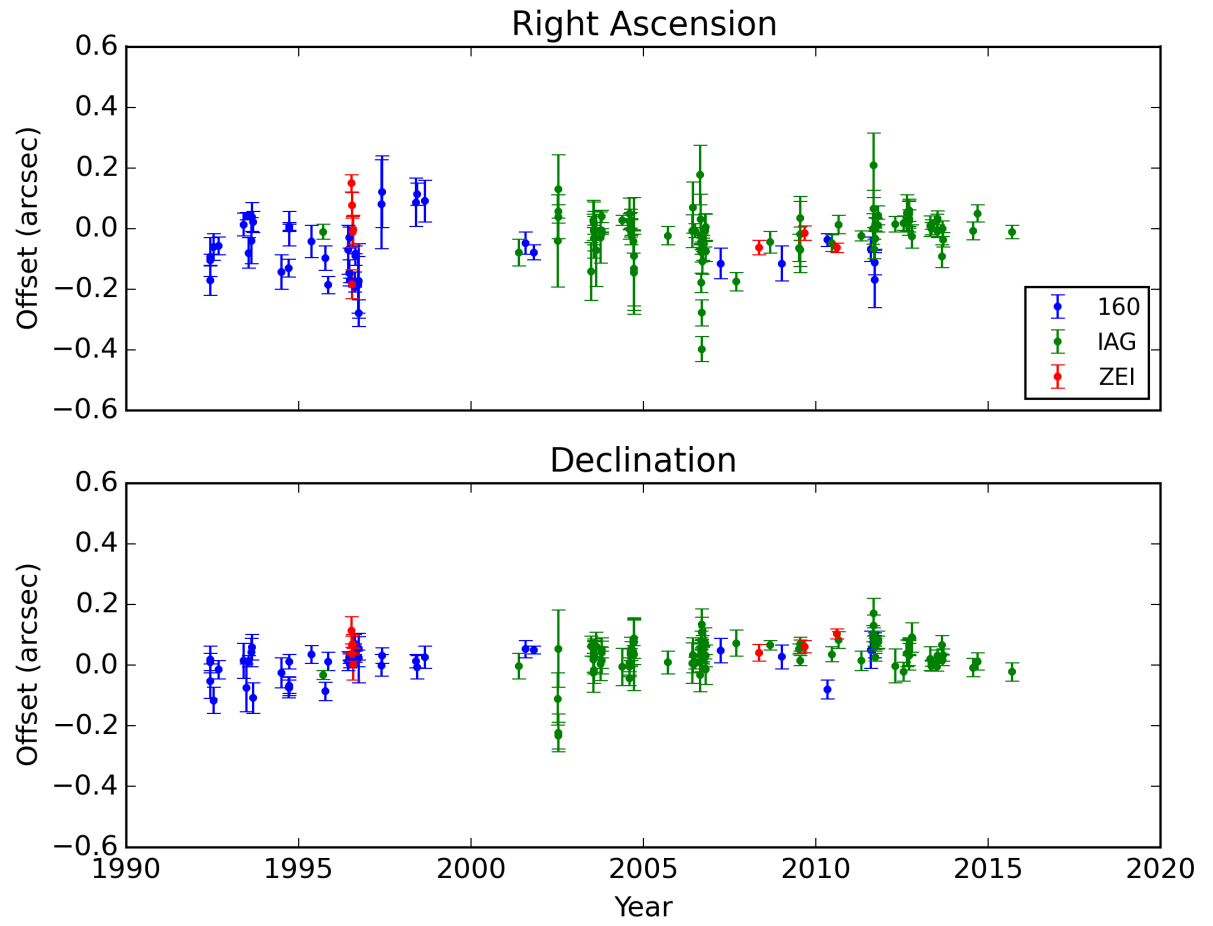


**Figure 13:** Difference between the offsets of Triton and Neptune - Mean offset by day

# Bibliography

- Benedetti-Rossi, G., Vieira Martins, R., Camargo, J. I. B., Assafin, M., and Braga-Ribas, F. (2014). Pluto: improved astrometry from 19 years of observations. *Astronomy & Astrophysics*, 570:A86.
- Pascu, D., Storrs, A. D., Wells, E. N., Hershey, J. L., Rohde, J. R., Seidelmann, P. K., and Currie, D. G. (2006). Hst bvi photometry of triton and proteus. *Icarus*, 185(2):487–491.
- Schmude, Jr., R. W., Baker, R. E., Fox, J., Krobusek, B. A., Pavlov, H., and Mallama, A. (2016). The Secular and Rotational Brightness Variations of Neptune. *ArXiv e-prints*.